# Free-running 2.4GHz Ring Oscillator-Based FSK TX/RX for Ultra-Small IoT Motes

David C. Burnett, Filip Maksimovic, Brad Wheeler, Osama Khan, Ali M. Niknejad, Kristofer S.J. Pister
University of California Berkeley, Berkeley, CA USA
{db, fil, brad.wheeler, oukhan, niknejad, pister}@eecs.berkeley.edu

***Abstract*— We demonstrate narrowband FSK communication between radios with free-running 2.4GHz ring oscillators requiring neither frequency synthesizer nor external frequency reference (e.g., crystal oscillator). After a single calibration and in an open lab environment, a free-running low-IF ring RX is able to demodulate coded binary FSK signals sent by a free-running ring TX (FSK tone separation 5.5MHz) with input power as low as -67dBm (yielding estimated 5.5m range) to better than 6.5% chip error rate (CER) / 1% packet error rate (PER) as specified by the IEEE 802.15.4 standard. By solely relying on ring oscillators for 2.4GHz tone generation, this work enables 600x chip area reduction when comparing a 10um x 10um ring oscillator (oscillator only, no current DAC) with a 250um x 250um 4.7nH LC tank (inductor only, no capacitor DAC). This work also enables 4x power reduction when comparing 105uW ring oscillator power vs. 400uW LC tank power.**

***Keywords*— Microwave integrated circuits, crystal free, crystalless, free running, ring oscillator, wireless sensor networks, smart dust.**

## I. Introduction

RF ring oscillators have the advantage of very small area and low power but are typically part of a large, power-hungry frequency synthesizer requiring an external crystal reference which negates the ring oscillator's advantages. Free-running ring oscillators are often found in digital systems as a compact low-power timing source. This is because digital circuits are intolerant to clock skew across the design but are tolerant to high variance at the clock edge's origin. But free-running ring oscillators are very seldom used in RF applications because of the difficulty in frequency tracking. In the frequency domain, their high phase noise leads to RF energy being "smeared" across a wide power spectral density. In the time domain, accumulated phase noise translates to jitter and makes frequency estimation difficult.

Local oscillator (LO) phase noise is traditionally considered in the context of interferers; by contrast, this work examines high phase noise effects on communication in the absence of nearby strong signals. We demonstrate communication between a 2.4GHz FSK transmitter and receiver, both of which operate without external crystal references and free from inductor-based oscillators, using only free-running deep submicron 2.4GHz ring LOs for tone generation. Eliminating inductors further enables RF design with digital synthesis tools instead of designing by hand. Most free-running ring oscillator work is comprised of uncertain-IF on/off keyed (OOK) wake-up radios [1]–[3], or very wideband (100s of MHz) FM-UWB frequency-shift keyed (FSK) TX [4] and RX [5]. Narrowband (<100MHz) free-running ring oscillator-based RF transceivers, communicating with each other (i.e., "peer-to-peer") instead of with a high-performance base station, were yet to be demonstrated until this work as compiled in Table 1. By leveraging ring oscillator size and power advantages, systems incorporating these ultra-small transceivers could have total form factor small/light enough to be suitable for: an unobtrusive skin implant to communicate physiological readings over a body-area network (BAN), the instrumentation of flying insects, or being added to chemical processing to make smart materials.

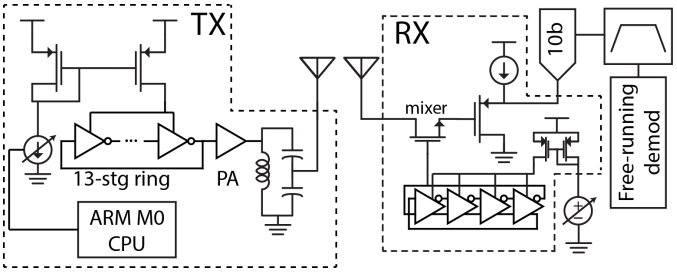


Fig. 1. System schematic for free-running transmitter & receiver.

## II. Implementation

This work consists of a 2.4GHz direct modulation transmitter and low intermediate frequency (IF) receiver using free-running ring LOs fabricated in TSMC 65nm CMOS. The system diagram is given in Fig. 1. To compensate for high phase noise/jitter, we communicate with a 2FSK-modulated, coded packet structure based on the IEEE 802.15.4 2.4GHz O-QPSK PHY. The packet is comprised of many 32-chip sequences, each representing 4-bit words, preceded by a Bluetooth LE-style 0x5555 preamble to aid windowed average initialization (windowed average described later in Sec. II-C). The RF LOs require no external components to operate besides power/bias. TX and RX LOs were manually calibrated to yield approximately 7MHz IF before several days of experiments. This calibration was performed as a substitute for system-level carrier search typically found in crystal-free radios [6]. Die photos of relevant components are shown in Fig. 2 with area values included in later sections to highlight relative size.

### A. Transmitter (TX)

The TX uses a 2.4GHz single-ended, 13-stage current-starved ring oscillator ($0.0009mm^2$) consuming

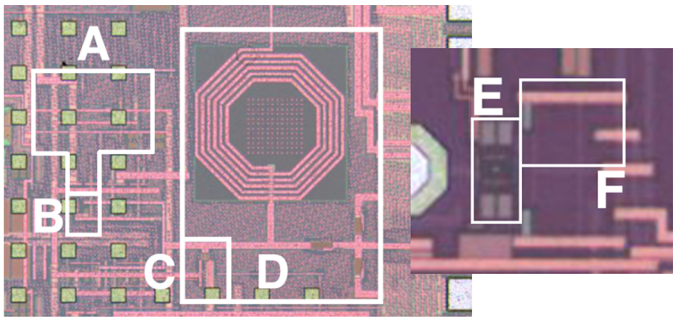


Fig. 2. Die photo showing (A) TX oscillator current bias network, (B) oscillator/mixer, (C) PA, (D) match, (E) RX: oscillator/mixer, (F) off-chip buffer. TX/RX dice not pictured to relative scale.

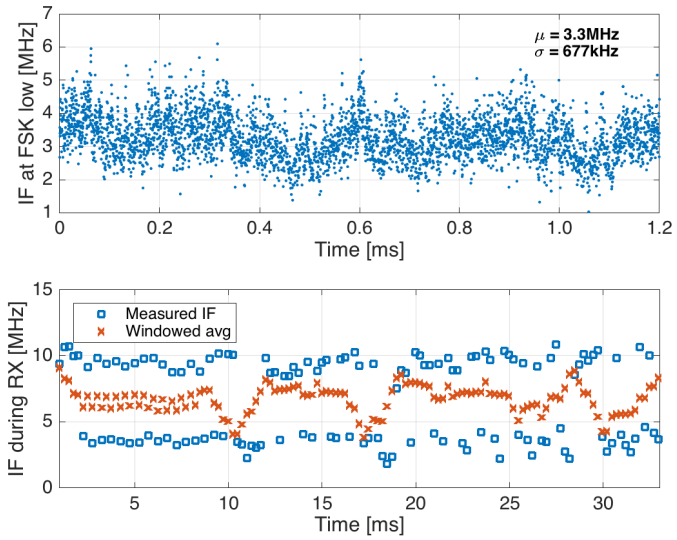


Fig. 3. (Top) Example of unmodulated IF over 1.2ms. In this example, the IF is approximately 3MHz because the transmitter is fixed at a frequency corresponding to a FSK zero. (Bottom) Modulated frequency measurements with moving average between.

364$\mu$W from 1.2V. Its RF output is amplified by a switching power amplifier (PA, 0.0013mm$^2$) consuming 1.6mW from 1.2V [7] and delivering $-12$dBm via tapped-capacitor passive on-chip match (0.1mm$^2$) to an external antenna. The oscillator is directly FSK modulated by adjusting its current DAC (0.053mm$^2$). Those adjustments are made by software running on an on-chip ARM Cortex M0 (1.23mm$^2$; includes 128kB SRAM).

Ring oscillators exhibit significant phase noise which manifests as significant frequency variance over time. An example of this variance is plotted in Fig. 3. This plot shows an IF resulting from a free-running ring oscillator TX mixed with a free-running ring oscillator RX. Because of this variance ($\sigma$ = 677kHz in the figure), FSK tone spacing in the transmitter was ~5.5MHz such that the demodulator could distinguish between noisy high and low frequency shifts with good chip error rate (CER). Fig. 4 shows the tradeoff between FSK tone spacing and CER when modulating with varying DAC codes.

To minimize jitter (and therefore FSK tone spacing) the

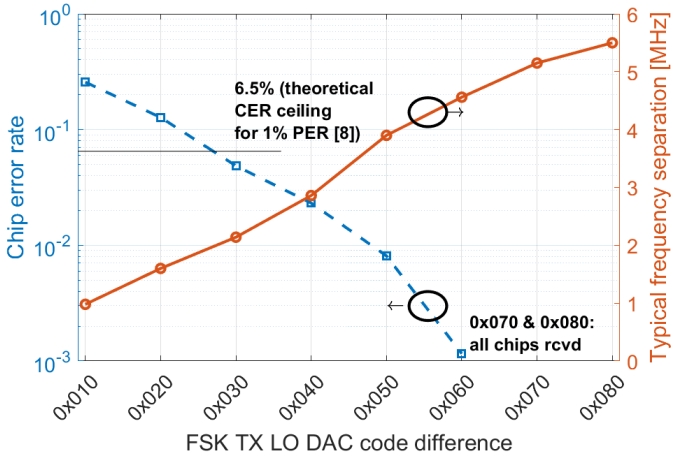


Fig. 4. Chip error rate, under high SNR to expose phase noise effects, and FSK frequency separation vs. TX DAC code separation.

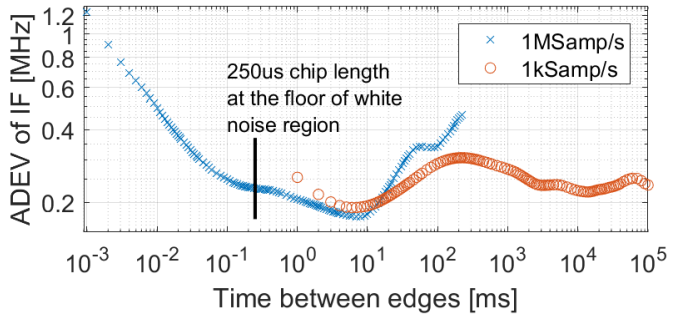


Fig. 5. Allan Deviation (ADEV) $\sigma_y(t)$ at IF resultant from free-running TX mixed with free-running RX.

bit period was chosen to be 250$\mu$s. This places the bit period at the "knee" between white & flicker frequency noise in the IF's Allan Deviation shown in Fig. 5. This "knee" is important because it is point at which flicker noise dominates with a flat ($\tau^0$) response. This prevents added averaging time from further decreasing time variance/jitter.

### B. *Receiver (RX)*

The RX uses a 2.4GHz differential, 4-stage current-starved ring oscillator (0.0006mm$^2$) consuming 105$\mu$W from 1V with current mirror tuned via off-chip voltage DAC as in [8]. To enable more flexible experimentation, RF input is fed directly to the passive NMOS mixer with neither passive match nor low-noise amplifier (LNA) at RF. Frontend gain is therefore estimated to be $-0.5$dB. The mixer gate is driven directly by the LO. The low intermediate frequency (Low-IF), 7MHz nominal, is buffered off-chip via PMOS source follower (0.014mm$^2$) for digitization and experimental demodulation. A simple 4-pole band-pass Butterworth filter with passband 2MHz to 32MHz is applied digitally before free-running demodulation.

### C. *Free-running demodulation*

The high phase noise/jitter inherent in ring oscillators makes traditional demodulation techniques, e.g., matched

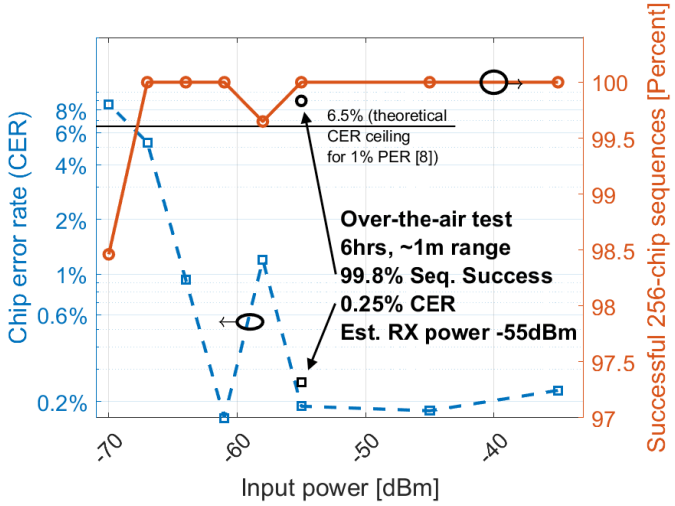


Fig. 6. Chip error rate (CER) and percent correctly de-correlated 256-chip (32-bit) sequences (1 - Packet Error Rate / 1-PER) vs. receiver input power.

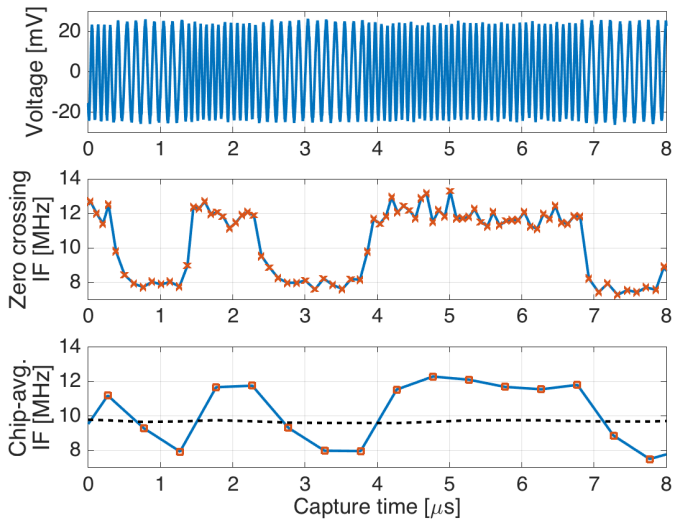


Fig. 7. Notional illustration of time-domain intermediate frequency (IF) voltage waveform, to frequency measured via zero-voltage crossings, to per-chip average frequency. Black dashed line in bottom figure is average of N past per-chip frequencies (typically 30). Note: transmitted frequency in this figure is 500x experimental bitrate for illustration purposes.

filters, perform poorly; as the free-running ring accumulates random error, the filter templates fail to match. Instead, we sample the IF using a 10-bit ADC at 100MS/s and measure current IF frequency by comparing zero crossing times. The external ADC timestamps samples with its own sense of time and such an integrated ADC could consume in excess of 1mW. Future work will time ADC with on-chip ring oscillators and investigate lower sampling rates & resolutions. A moving average of recent per-chip frequency measurements (typically 30 measurements of 250$\mu s$ bit periods forming a 7.5ms window) follows the IF drift over time and average frequency over the last chip period is compared with the moving average to determine binary value (Fig. 7).

Bit alignment via clock/data recovery is assumed for our purposes and is outside the scope of this jitter-focused work. The IF is acquired for data length plus 12% guard time at 18s intervals in 256-chip (32-bit) blocks. When a 32-chip 802.15.4-style preamble is recognized, we de-correlate subsequent chips in groups of 32 using 802.15.4 codes (converted from O-QPSK to FSK) to recover data. Separately, we compare the recovered chips and with original data to calculate CER (Figs. 4, 6).

## III. Performance

TX and RX local oscillators were tuned once manually to 2.45GHz before several days of measurement. Temperature was not controlled except insofar as the ambient lab environment is regulated by building controls. TX output was attenuated inline and fed into receiver. All data is resultant from free-running TX mixed down by a free-running RX. Comparing ADEV @ 1.2ms in Fig. 5 with $\sigma$=677kHz in Fig. 3 we see ADEV jitter estimates are conservative. The cumulative distribution function (CDF) tells us we need FSK tone separation >1.03MHz (code 0x010), given $\sigma$=677kHz, for 6.5% CER (target from [9]). Experiment shows 2.1MHz (code 0x030) is the minimum necessary in high SNR conditions (Fig. 4). In practice we widened FSK tones to the point of diminishing returns at low input powers (e.g., −67dBm sensitivity is not improved for FSK separations >5.5MHz, code 0x080) adding ~3.4MHz BW for ~+15dB sensitivity.

A more developed implementation would substitute a carrier search algorithm for our one-time manual tuning [6]. Our free-running rings exhibit too much noise to listen to typical standards-compliant radios but standard WiFi has been demonstrated to transmit FSK with 4MHz tone separation [10], which is within this work's capability. Sensitivity for 4MHz tone separation is given Fig. 4 and assumes a free-running transmitter. We expect $<10^{-3}$ CER when listening to a WiFi-generated beacon. Once calibrated, drift can be corrected for whenever a packet is exchanged.

### A. Temperature drift concerns

A representative RF ring oscillator was cycled 0 to 70°C Fig. 8. From this test we know temperature sensitivity across the 2.4GHz ISM band is ~7MHz/°C. A fully on-chip (internal ADC, etc.) implementation will have limited bandwidth (BW) to keep baseband power and noise BW low. We state 30MHz of IF BW in Table 1 given the Butterworth filters but, given our IF modulation width of 5.5MHz and IF $\sigma$ of 0.677MHz, our true BW requirement is likely closer to 3$\sigma$+5.5MHz+3$\sigma$=9.5MHz. Our ring oscillator will drift 9.5MHz/2 with temperature change of <0.7°C; hence, closer attention to temperature drift may be necessary depending on future power/sensitivity tradeoffs. When the system experiences temperature drift, we will rely on IF measurement to periodically measure the average IF value and adjust the current DAC to keep up with temperature drift as demonstrated in [6], [7]. A simple low-power on-chip RC oscillator is an appropriate reference for this coarse IF measurement. Packet exchange corrections must occur more frequently than the environmental drift rate.

Table 1. Comparison to all other known published works incorporating free-running ring oscillators.

| | This work | [1] Milosiu WiSNet 2015 | [2] Pletcher ISSCC 2008 | [3] Bryant ESSCIRC 2014 | [4] Saputra JSSC 2011 | [5] Kopta RFIC 2016 |
|---|---|---|---|---|---|---|
| Frequency | 2.4GHz | 2.4GHz | 2.0GHz | 2.4GHz | 4.0GHz | 4.0GHz |
| Process | 65nm | 130nm | 90nm | 90nm | 90nm | 65nm |
| Ring Oscillator Topology | 4-stage differential RX 13-stg single-ended TX | Not reported | 3-stage single | 3-stage single | 3-stage single | 2-stage differential |
| Modulation | FSK | OOK | OOK | OOK | FM-UWB | FM-UWB |
| Data rate | 4kcps (0.5kbps) | up to 33kbps | 100kbps | 250kbps | 100kbps | 100kbps |
| Bandwidth | 30MHz | 100MHz (est.) | 100MHz | 54MHz | 500MHz | 300MHz |
| Oscillator Power | 105$\mu$W RX; 364$\mu$W TX | up to 233$\mu$W | 6$\mu$W | 13$\mu$W | 280$\mu$W | 140$\mu$W |
| Off-chip RF components? | None | (Unknown) | BAW RF Filter | None | Match | None |
| Chip-to-chip communication? | Yes, TX/RX | Wakeup RX only | Wakeup RX only | Wakeup RX only | TX only | RX only |
| Sensitivity | $-$67dBm for 6.5% CER, 1% PER | $-$80dBm for 1% wakeup word error | $-$72dBm for $10^{-3}$ BER | $-$88dBm for $10^{-3}$ BER | N/A (TX only) | $-$70dBm for $10^{-3}$ BER |

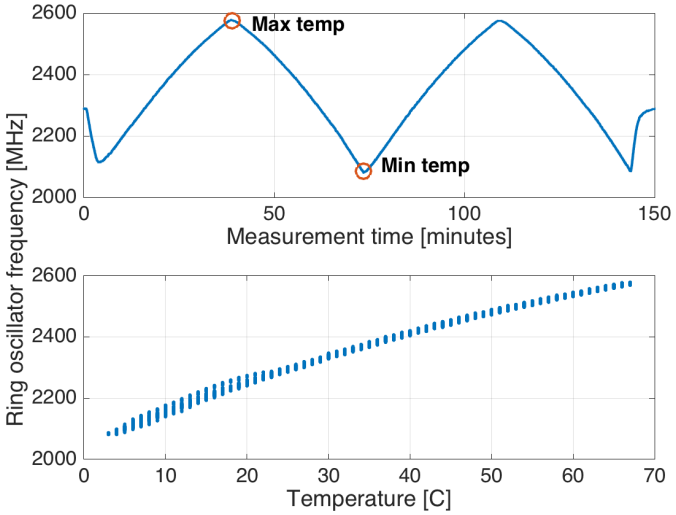


Fig. 8. Frequency changes in response to changing temperature for a representative RF ring oscillator. Temperature measured by thermocouple temperature probe included with a MAS-345 multimeter retrieved via serial.

## IV. Conclusion

We have demonstrated FSK communication between a 2.4GHz RF transmitter and receiver, each with local oscillators consisting only of 2.4GHz free-running ring oscillators requiring no FLL/PLL or external frequency (crystal) reference. While other free-running ring work assumes communication with a crystal-based node, this work instead demonstrates "peer-to-peer" communication. The receiver in this work was kept simple for experimental flexibility so significant performance improvements may be realizable with modest RX improvements, e.g., LNA and IF gain. We see acceptable performance ($<$6.5% CER, $<$1% Packet Error Rate/PER) down to $-$67dBm (Fig. 6). Beyond that point, IF amplitude falls below the noise floor of our off-chip ADC. This corresponds to $-$55dB attenuation (5.5m estimated range), demonstrating potential for complete ultra-small RF transceivers to occupy $<$0.1mm$^2$ die area and enabling a new size threshold of wireless sensing.

## Acknowledgment

We thank the students, faculty, and sponsors of the Berkeley Wireless Research Center (BWRC) and the Berkeley Sensor & Actuator Center (BSAC). Work was supported by the Department of Defense (DoD) through the National Defense Science and Engineering Graduate (NDSEG) Fellowship.

## References

[1] H. Milosiu, F. Oehler, M. Eppel, D. Früehsorger, and T. Thöenes, "A 7-$\mu$W 2.4-GHz wake-up receiver with -80 dBm sensitivity and high co-channel interferer tolerance," in *2015 IEEE Topical Conference on Wireless Sensors and Sensor Networks (WiSNet)*, Jan. 2015, pp. 35–37.

[2] N. M. Pletcher, S. Gambini, and J. M. Rabaey, "A 2GHz 52 $\mu$W Wake-Up Receiver with -72dBm Sensitivity Using Uncertain-IF Architecture," in *2008 IEEE ISSCC*, Feb. 2008, pp. 524–633.

[3] C. Bryant and H. Sjöland, "A 2.45GHz, 50$\mu$W wake-up receiver front-end with -88dbm sensitivity and 250kbps data rate," in *2014 ESSCIRC 2014 - 40th European Solid State Circuits Conference*, Sep. 2014, pp. 235–238.

[4] N. Saputra and J. R. Long, "A Fully-Integrated, Short-Range, Low Data Rate FM-UWB Transmitter in 90 nm CMOS," *IEEE Journal of Solid-State Circuits*, vol. 46, no. 7, pp. 1627–1635, Jul. 2011.

[5] V. Kopta, D. Barras, and C. C. Enz, "A 420 $\mu$W, 4 GHz approximate zero IF FM-UWB receiver for short-range communications," in *2016 IEEE RFIC Symposium*, May 2016, pp. 218–221.

[6] I. Suciu, F. Maksimovic, D. Burnett, O. Khan, B. Wheeler, A. Sundararajan, T. Watteyne, X. Vilajosana, and K. Pister, "Experimental clock calibration on a Crystal-Free Mote-on-a-Chip," in *IEEE INFOCOM WKSHPS: CNERT 2019*, Paris, France, Apr. 2019.

[7] F. Maksimovic, B. Wheeler, D. C. Burnett, O. Khan, S. Mesri, I. Suciu, L. Lee, A. Moreno, A. Sundararajan, B. Zhou, R. Zoll, A. Ng, T. Chang, X. Villajosana, T. Watteyne, A. Niknejad, and K. S. J. Pister, "A Crystal-Free Single-Chip Micro Mote with Integrated 802.15.4 Compatible Transceiver, sub-mW BLE Compatible Beacon Transmitter, and Cortex M0," in *2019 VLSI Symposium*, Jun. 2019, pp. C88–C89.

[8] D. C. Burnett, B. Wheeler, F. Maksimovic, O. Khan, A. M. Niknejad, and K. S. J. Pister, "Narrowband communication with free-running 2.4GHz ring oscillators," in *IEEE PEMWN Conference*, Nov. 2017, pp. 1–6.

[9] O. Khan, B. Wheeler, F. Maksimovic, D. Burnett, A. M. Niknejad, and K. Pister, "Modeling the Impact of Phase Noise on the Performance of Crystal-Free Radios," *IEEE Transactions on Circuits and Systems II: Express Briefs*, vol. 64, no. 7, pp. 777–781, Jul. 2017.

[10] Y. Dai, W. Peng, Y. Wang, L. Chuo, K. Suri, H. Zheng, D. Wentzloff, and H. Kim, "Implementation and Evaluation of Bi-Directional WiFi Back-channel Communication," in *2018 IEEE 29th Annual PIMRC Symposium*, Sep. 2018, pp. 1–7.